ISSN 0031-918X, The Physics of Metals and Metallography, 2016, Vol. 117, No. 12, pp. 1245–1250. © Pleiades Publishing, Ltd., 2016.
Original Russian Text © O.A. Chikova, P.L. Reznik, B.V. Ovsyannikov, 2016, published in Fizika Metallov i Metallovedenie, 2016, Vol. 117, No. 12, pp. 1296–1301.

STRUCTURE, PHASE TRANSFORMATIONS, AND DIFFUSION

Structure and Nanomechanical Characteristics of Al–Cu–Mg–Si Alloy with Partly Liquated Grain Boundaries upon Heat Treatment

O. A. Chikova[a, *], P. L. Reznik[a], and B. V. Ovsyannikov[b]

[a] *Yeltsin Ural Federal University, ul. Mira 19, Ekaterinburg, 620002 Russia*

[b] *OAO Kamensk-Uralsky Metallurgical Works, ul. Zavodskaya 5, Kamensk-Uralskiy, Sverdlovskaya oblast, 623405 Russia*

**e-mail: Chik63@mail.ru*

Received March 22, 2016; in final form, July 12, 2016

Abstract—The microstructure, phase composition, and mechanical characteristics of the structural constituents of an Al–Cu–Mg–Si alloy in which the liquation of grain boundaries occurred during heat treatment have been studied. Bands of the $(Al + Al_{15}(Fe, Mn)_3Si_2)$ eutectics have been observed at the grain boundaries. An algorithm for calculating the additional pressure, which results from mechanical impact on the metal containing these bands has been described.

Keywords: microstructure, nanoindentation, hardness, Young's modulus, liquation of grain boundaries, heat treatment, Al–Cu–Mg–Si aluminum-based alloy

DOI: 10.1134/S0031918X16120036

INTRODUCTION

Semifinished products of an AK6 aluminum-based alloy of the Al–Cu–Mg–Si system have become popular in aircraft construction and other industries [1, 2]. This alloy has the following chemical composition: 0.6 wt % Mg, 1.0 wt % Si, 2.3 wt % Cu, 0.6 wt % Mn, 0.1 wt % Ti, 0.1 wt % Zn, 0.2 wt % Fe, 0.1 wt % Ni, and α-Al makes up the balance. According to the literature data, the chemical composition of the AK6 alloy is represented by the following phases: the aluminum-based alpha solid solution (α-Al), as well as aluminides $CuAl_2$, Al_2CuMg, $Al_5Cu_2Mg_8Si_6$, and $Al_{15}(Fe, Mn)_3Si_2$. Silicon and iron impurities form eutectics in aluminum, which consists of the aluminum-based solid solution and Al_5FeSi crystals with the typical Chinese-character morphology [3, 4]. To neutralize the harmful effect of iron, aluminum-based alloys are added with manganese, which favors the formation of the $Al_{15}(Fe, Mn)_3Si_2$ compound; this compound undergoes primary solidification from a melt to form small edged crystals, which enhances the ductility of an alloy. The $Al_{15}(Fe, Mn)_3Si_2$ eutectic phase is made up of iron in the amount of 1.2–2.2 wt % and manganese in the amount of 0.2–1.2 wt % [3–8]. A decrease in the concentration of the $Al_{15}(Fe, Mn)_3Si_2$ phase to less than 3 vol % leads to the deterioration of the ductility characteristics [6]. Upon standard heat treatment, $Al_{15}(Fe, Mn)_3Si_2$ crystals coagulate during the subsequent cooling and the solidification of the molten eutectics due to an excess of free surface energy to form coarse inclusions with typical skeletal morphology [9].

Semifinished products of an AK6 aluminum-based alloy are supplied in the heat-treated state. The maximum strengthening of the AK6 alloy is achieved using quenching and artificial aging. In order to achieve the most complete dissolution of proeutectoid constituents, parts made of AK6 alloy are quenched in a temperature range of 495–500°C; these temperatures are close to the solidus temperature, which is determined by the temperature of the most fusible eutectics $CuAl_2 + Al_5Cu_2Mg_8Si_6 + Al_2CuMg$, i.e., 505°C. When ingots of the AK6 alloy are produced, the liquation of the eutectics followed by its solidification is observed fairly often. This effect is called *bursting* [10], and it leads to the deterioration of the mechanical characteristics of the alloy and is considered to be an undesirable phenomenon in the production of aluminum-based alloys.

The aim of this work was to study the microstructure, phase composition, and mechanical characteristics of the structural constituents of the AK6 alloy in which the partial liquation of grain boundaries has occurred in the course of homogenization for 12 h at a temperature of 502 ± 2°C, i.e., in which signs of bursting have been observed. Furthermore, the additional pressure that arises during mechanical impact on the alloy due to the presence of eutectic aluminides at the grain boundaries, which have Young's modulus that differs from that of the matrix, has been estimated.

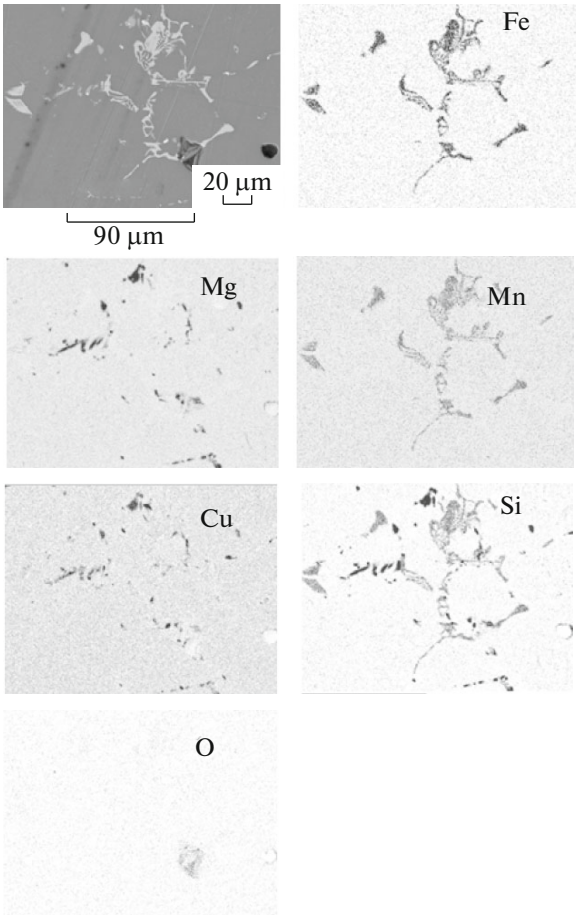

Fig. 1. SEM-micrographs of the microstructure of the AK6 alloy specimen with the signs of bursting and chemical element maps obtained using EDS.

EXPERIMENTAL

The objects of the study were specimens fabricated from the middle zone of a heat-treated AK6 alloy ingot 377 mm in diameter, which exhibited signs of the liquation of grain boundaries. The microstructure of the alloy was examined using traditional quantitative metallography methods implemented in a JSM-5900 LV scanning electron microscope. The energy dispersive X-ray spectroscopy (EDS) of the phases in the ingot was carried out with a relative error of determining the concentration of chemical elements of 5% at concentrations of the elements less than 10% and 1% at concentrations of the elements more than 10%. Phase analysis was performed using a Bruker D8 Advance X-ray diffractometer; the experimental data were processed using FULLPROF general-purpose software supplemented with WinPLOTR graphic toolset. The Meyer hardness *HM* (GPa) and Young's modulus *E* (GPa) were measured in submicron-sized volumes of the AK6 alloy ingot. The hardness *HM* and Young's modulus *E* were measured using nanoindentation implemented in a NanoScan-4D scanning nanohardness tester. Noise on the frequency curve, which arises when the indenter contacts the surface of the alloy, is equal to ~1 μN and 0.3 nm, while the maximum scatters of the load and the displacement are equal to 1 N and 700 μm, respectively. The limits of the permissible fundamental relative error of the applied load are equal to ± 10 μN (± 1%). The measurements of the nanomechanical characteristics of the AK6 alloy ingot using nanoindentation were carried out in accordance with the requirements of the international standard ISO 14577 and the Russian standard GOST 8.748–2011. The hardness and Young's modulus were measured at room temperature under the continuous loading of the specimens by a linearly increasing load. The loading and unloading of the indenter, as well as the recording of the *P*–*h* curve, which is the dependence of the applied load on the depth of indentation, were automatically implemented. The size of the impression was determined by measuring the maximum depth of indentation h_{max}. The maximum size of the impression produced under a load of 1 mN is equal to 200 nm. The test results were processed using the Oliver–Pharr method [11]. The microhardness was calculated as the ratio of the maximum load to the area of the projection of the unrecovered impression $HM = \frac{P}{F}$, where P was the load applied to the indenter; $F = 24.56h_c^2$ was the area of the projection of the impression on the surface of the specimen; and h_c was the depth of the unrecovered impression. The Meyer hardness *HM* determined in this way is equal to the average pressure on the indenter–specimen interface [12, 13]. The disk specimens were mechanically and electrolytically polished to achieve an asperity height of no more than 10 nm.

RESULTS

Figure 1 shows the microstructure and the elemental composition of the cast AK6 alloy with liquated grain boundaries upon heat treatment. The X-ray diffraction phase analysis of the specimens has identified the following phases: alpha aluminum, Al_2Cu, $Al_5Cu_2Mg_8Si_6$, and Al_2CuMg. With account for the EDS data and the results reported in [5–8], the presence of the $Al_{15}(Fe, Mn)_3Si_2$ phase in the (α-Al + $Al_{15}(Fe, Mn)_3Si_2$) eutectics was assumed [9]. At the grain boundaries of alpha aluminum, not only inclusions of the $Al_{15}(Fe, Mn)_3Si_2$ phase with the typical skeletal morphology, but also inclusions of the $Al_5Cu_2Mg_8Si_6$ with the edged morphology, are observed (Fig. 1). The volume fraction of $Al_{15}(Fe, Mn)_3Si_2$ crystallites is five to seven times larger than that of $Al_5Cu_2Mg_8Si_6$ crystallites. We also note that the alloy subjected to heat treatment contains discontinuity flaws, the surfaces of which are enriched in oxygen, which is presumably contained in aluminum oxide Al_2O_3 (Fig. 1).

In order to assess the effect of the liquation of grain boundaries on the mechanical characteristics of the AK6 alloy with signs of bursting, its nanomechanical characteristics, i.e., the nanohardness and Young's modulus, were measured in submicron-sized volumes of that alloy. The measurements of *HM* and *E* were carried out along the 90-μm long indentation line, which was drawn through a bursting (α-Al + $Al_{15}(Fe, Mn)_3Si_2$) eutectic inclusion and an α-Al dendrite, with a step of 2 μm.

The results of measuring the mechanical characteristics (*E*, GPa and *HM*, GPa) of the structural constituents of the AK6 alloy with partly liquated grain boundaries are presented in Fig. 2 and the table. These results agree with the following data obtained in [14] for Al (99.5%): $E = 70 \pm 3$ GPa and $HM = 0.6 \pm 0.1$ GPa. The Meyer hardness of alpha aluminum in the alloy under study ($HM = 2$ GPa), which is higher than that of A1 (99.5%), can be explained by the solid-solution hardening of this alloy [15, 16].

We note the scatter of the values of *E* and *HM* in the zone of the eutectic inclusion. The maximum values of Young's modulus ($E \approx 150$ GPa) and the Meyer hardness ($HM \approx 10$ GPa) measured for the eutectic inclusion are close to those obtained in [17] for Si ($E = 150$ GPa and $HM = 11.85$ GPa) and the $A1_3Fe$ compound ($E = 110$ GPa and $HM = 7.81$ GPa). Substantial variations in *HM* from 10 to 2 GPa, which corresponds to the value of *HM* for alpha aluminum, observed within the bursting inclusion can be related to the presence of microzones of alpha aluminum within the complex-shaped skeletal inclusion of the intermetallic compound. It is also known that the strength of a material is inversely proportional to the scatter of values of *HM* and *E* [18]. Therefore, the bursting eutectic inclusion is characterized by the reduced strength and can be considered as a potential fracture nucleus during the mechanical loading of the part.

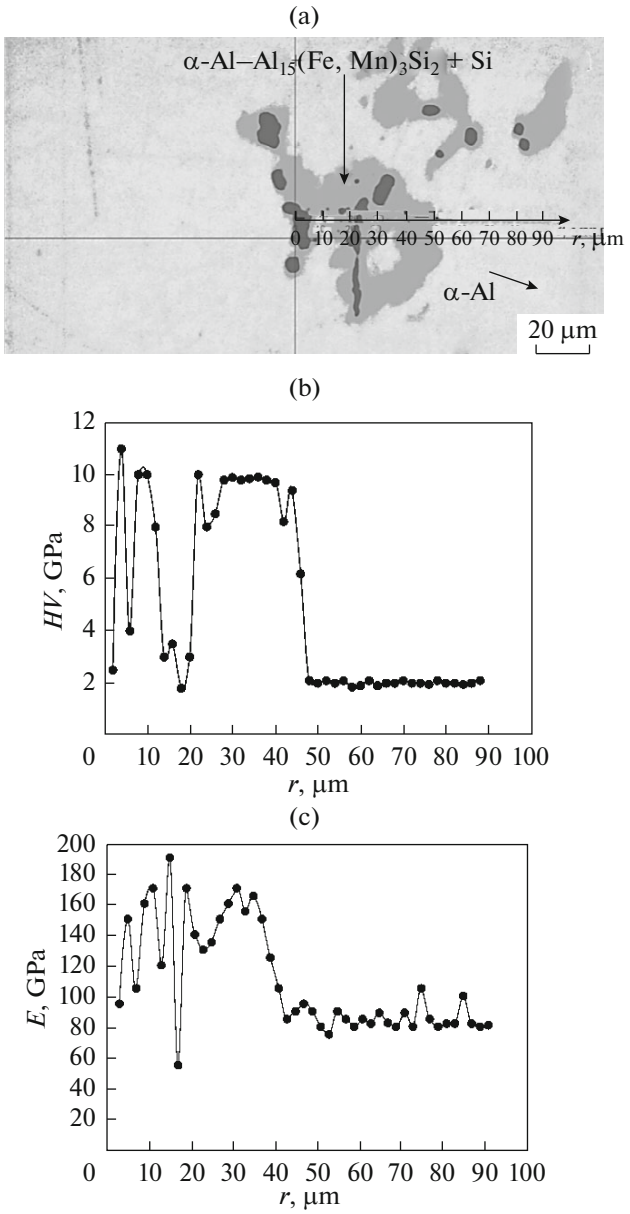

Fig. 2. Nanomechanical characteristics of the cast AK6 alloy: (a) indentation profile; (b) distribution of nanohardness *HM* along indentation line; and (c) distribution of Young's modulus *E* along indentation line.

DISCUSSION

The majority of researchers attribute the partial liquation of grain boundaries due to the homogenization of an AK6 alloy ingot to the melting of the eutectics ($CuAl_2$ + $Al_5Cu_2Mg_8Si_6$ + Al_2CuMg), which occurs during the heating of the ingot to a temperature of 505°C in the course of heat treatment [3–7]. It was assumed in [9] that alloys for which the chemical compositions were similar to the chemical composition of the AK6 alloy two eutectics, i.e., (α-Al + Cu_2Al + Mg_2Si) and (α-Al + $Al_{15}(Fe, Mn)_3Si_2$), simultaneously existed at grain boundaries. It is known that the crystallization-induced $Al_{15}(Fe, Mn)_3Si_2$ phase can be simultaneously present both at the grain boundaries and in the bulk of alpha-aluminum dendrites. The $Al_{15}(Fe, Mn)_3Si_2$ crystallites localized at the grain boundaries have the bcc lattice; dispersoids that have identical stoichiometric compositions but simple cubic lattices are distributed over the bulk of the aluminum matrix [19, 20]. The EDS results (Fig. 1) have shown that two fusible eutectics, i.e., (α-Al + $Al_5Cu_2Mg_8Si_6$) and (α-Al + $Al_{15}(Fe, Mn)_3Si_2$), are present at the grain boundaries.

The decrease in the strength of the AK6 alloy ingot is attributed to the appearance of elongated inclusions of the eutectic composition due to the liquation of the grain boundaries [8, 10]. The authors of these works believe that, in this case, the cause of the decrease in the strength of the alloy is the nonuniformity of its elastic characteristics. A mechanical impact on the

Results of measuring the mechanical characteristics of the structural constituents of the AK6 alloy

	h_{max}, nm	h_{res}, nm	HM, GPa	R	E, GPa	E^*, GPa	HM/E^*	HM^3/E^{*2}
Matrix (α-Al)	218	184	2	0.16	70	80	0.0248	0.0012
Inclusion contained in eutectics	118	76	10	0.36	150	172	0.0575	0.0327

material containing inclusions Young's modulus of which differs from that of the matrix results in an additional pressure P_r [21]. The pressure P_r resulted from the mechanical impact of the stresses induced by the inhomogeneity of the specimen on the AK6 alloy was estimated using the nanoindentation data (Fig. 2). It was assumed that the specimen consisted of an α-Al matrix and eutectic (α-Al + $Al_{15}(Fe, Mn)_3Si_2$) inclusions (Fig. 1). Young's moduli of the matrix and an inclusion were determined as average values of the nanoindentation data, which were equal to E_{Al} = 70 GPa and E_{incl} = 150 GPa, respectively (Fig. 2). The additional pressure P_r, which arises under the mechanical loading of the ingot by the force F, can be calculated using the following formula [22]:

$$P_r = \frac{4\varepsilon\mu\mu_0}{R(2\mu_0 + \mu(\chi_0 - 1))}, \quad (1)$$

where

$$\varepsilon = \frac{F}{4\pi R^2}\left(\frac{1}{E} - \frac{1}{E_0}\right); \quad (2)$$

$$\chi_0 = \frac{\lambda_0 + 3\mu_0}{\lambda_0 + \mu_0}, \quad (3)$$

λ and μ are the Lame constants; R is the radius of the inclusion; and F is the external force. The subscript 0 means the characteristics of the inclusion.

In our case, λ_0 = 45.45 GPa, λ = 60.80 GPa, μ_0 = 24.7 GPa, and μ = 28.3 GPa [15, 23, 24]. The calculation has shown that the additional pressure P_r, which results from the difference between Young's moduli of the matrix and the inclusion, is 162 times higher than the external force F. Therefore, the pressure P_r can be a cause of the fracture of the material during machining.

When tensile stresses F act on a specimen with an inclusion along the OX axis, the following stress state arises in this specimen [22]:

$$X_x^0 = F\frac{\beta_0 + \delta_0}{2}; \quad (4)$$

$$Y_Y^0 = F\frac{\beta_0 - \delta_0}{2}; \quad (5)$$

$$X_Y^0 = 0, \quad (6)$$

where

$$\beta_0 = \frac{\mu_0(\chi + 1)}{2\mu_0 + \mu(\chi_0 - 1)}; \quad (7)$$

$$\delta_0 = \frac{\mu_0(\chi + 1)}{\mu + \mu_0\chi_0}. \quad (8)$$

The calculation has shown that the mechanical stresses that arise in the inclusion do not exceed 0.45F, which also indicates that the additional pressure P_r, which results from the difference between Young's moduli of the α-Al matrix and the eutectic (α-Al + $Al_{15}(Fe, Mn)_3Si_2$) inclusion, is the governing factor of the fracture of the alloy.

The Meyer hardness HM is equal to the mean contact pressure at the indenter–specimen interface and correlates well with the flow stress [25]. If the values of E and HM are known, the ductility characteristic of the material δ_A can be estimated [17]. The ductility characteristic δ_C determined by continuous indentation is an analog of the dimensionless ductility parameter δ_C, which is the fraction of the plastic deformation in the total elastoplastic deformation under the indenter and characterizes the capacity of the material for forming during deformation; this characteristic can be calculated as follows:

$$\delta_C = 1 - 10.2(1 - \nu - \nu^2)\frac{HM}{E}, \quad (9)$$

where ν is Poisson's ratio. It follows from this formula that the ductility characteristic δ_C is primarily determined by the ratio $\frac{HM}{E}$ and that, with an increase in the hardness of the material and at constant Young's modulus E, the ductility characteristic should decrease. The decrease in the ductility characteristic with increasing hardness should be promoted if Young's modulus simultaneously decreases. The theoretical and experimental results presented in [25] have shown that with the specified degree of accuracy it can be taken that $\delta_C = \delta_A$. The results of estimating data on variations in HM and E of the cast AK6 alloy are presented in Fig. 2. These results show that, in passing from the inclusion of the eutectic (α-Al + $Al_{15}(Fe, Mn)_3Si_2$) to the α-Al matrix, the ratio $\frac{HM}{E}$ decreases by half. Therefore, the ductility characteris-

tic $\delta_C = \delta_A$ increases, which correlates with the change in the Meyer hardness *HM*.

The parameters $\frac{HM}{E^*}$ and $\frac{HM^3}{E^{*2}}$, where $E^* = \frac{E}{1-\nu^2}$ is the contact modulus of elasticity, were also calculated using the nanoindentation data [26]. The ratios $\frac{HM}{E^*}$ and $\frac{HM^3}{E^{*2}}$ characterize the specific contact hardness of the material and its resistance to plastic deformation. These parameters determine the capacity of the material for withstanding mechanical loads without residual deformation. The ratio $\frac{HM}{E^*}$ also substantially decreases in passing along the indentation line from the eutectic (α-Al + $Al_{15}(Fe, Mn)_3Si_2$) inclusion to the α-Al matrix (the table).

An analysis of the continuous loading diagram provides information on the hardness of the material, as well as makes it possible to estimate the fractions of the elastic and plastic deformations in the total elastoplastic deformation under the indenter [12]. The fraction of the elastic component in the total deformation is characterized by the elastic recovery $R = \frac{h_{max} - h_{res}}{h_{max}}$, where h_{max} is the maximum depth of indentation and h_{res} is the residual depth or the depth of the impression upon unloading. The results of analysis of the relation between the characteristics of the indentation curve and the mechanical characteristics of the material, which is presented in the form of the equation of indentation $HM \approx \left(\frac{1}{R} - 1\right)$, have shown that, the greater the elastic recovery *R*, the lower the hardness (table) [21, 26]. Thus, in passing along the indentation line from the inclusion of the eutectic (α-Al + $Al_{15}(Fe, Mn)_3Si_2$) to the α-Al matrix, the elastic recovery of the material *R* decreases by approximately four times.

CONCLUSIONS

In order to identify causes of the fracture of the ingot of the AK6 alloy with partly liquated grain boundaries under mechanical loading, the microstructure, phase composition, and mechanical characteristics of the structural constituents of the alloy have been studied.

The use of EDS has made it possible to identify the following phases: α-Al, Al_2Cu, $Al_5Cu_2Mg_8Si_6$, and Al_2CuMg. Extended areas enriched in silicon, manganese, and iron that contain inclusions of the $Al_{15}(Fe, Mn)_3Si_2$ phase have been observed at the grain boundaries. Using the EDS data, it has been assumed that two fusible eutectics, i.e., α-Al + Cu_2Al + Mg_2Si and α-Al + $Al_{15}(Fe, Mn)_3Si_2$, are present at the grain boundaries. Young's modulus *E* and the Meyer hardness *HM* have been measured along the line that passes through the inclusion of the fusible (Al + $Al_{15}(Fe, Mn)_3Si_2$) eutectics and the α-Al matrix.

The calculation assessment of the additional pressure P_r, which arises at the inclusion–matrix interface due to the loading of the material by an external force, has been carried out. The pressure P_r results from the difference in the moduli of elasticity of the inclusion and the matrix. The calculation has shown that additional pressure at the (Al + $Al_{15}(Fe, Mn)_3Si_2$) inclusion–α-Al matrix interface is 162 times higher than the external force.

It has been found that, in passing along the indentation line from the eutectic (α-Al + $Al_{15}(Fe, Mn)_3Si_2$) inclusions [16] to the α-Al matrix the ratio $\frac{HM}{E}$ decreases by half; therefore, the ductility characteristic of the material δ_A increases, which correlates with the change in the Meyer hardness *HM*. In passing from the inclusion of the eutectic (α-Al + $Al_{15}(Fe, Mn)_3Si_2$) to the α-Al matrix, the elastic recovery of the material *R* decreases by four times.

ACKNOWLEDGMENTS

This work was carried out in accordance with the state assignment of the Ministry of Education and Science of Russian Federation, contract no. 3.1236.2014/K.

REFERENCES

1. Aluminum. Properties and Physical Metallurgy. A Handbook, Ed. by J. E. Hatch (ASM, Ohio, 1984; Metallurgiya, Moscow, 1989).
2. L. F. Mondol'fo, Aluminum Alloys: Structure and Properties (Butterworth, London, 1976; Metallurgiya, Moscow, 1979).
3. N. A. Belov, Phase Content of Industrial and Perspective Aluminum Alloys (MISiS, Moscow, 2010) [in Russian].
4. X. Cao and J. Campbell, "Morphology of β-Al5FeSi phase in Al–Si cast alloys," Mater. Trans., **47**, 1303–1312 (2006).
5. S. Seifeddine and I. L. Svensson, "The influence of Fe and Mn content and cooling rate on the microstructure and mechanical properties of A380-die casting alloys," Metall. Sci. Techn., **27**, 11–20 (2009).
6. M. Tash, F. H. Samuela, F. Mucciardic, and H. W. Doty, "Effect of metallurgical parameters on the hardness and microstructural characterization of as-cast and heat-treated 356 and 319 aluminum alloys," Mater. Sci. Eng., A **443**, 185–201 (2007).
7. V. D. Belov, A. G. Tsydenov, S. B. Novichkov, S. V. Savchenko, A. G. Stroganov, and N. A. Belov, RF Patent 2415193 (2011).
8. N. V. Kazennov, K. B. Kalmykov, S. F. Dunaev, and N. E. Dmitrieva, "Phase equilibria in the Al–Mn–Si system at 823 K," Metal Sci. Heat Treat. **53**, 113–117 (2011).

9. H. L. Moraes, J. R. Oliveira, D. Espinosa, and J. A. Tenorio, "Removal of iron from molten recycled aluminum through intermediate phase filtration," Mater. Trans. **47**, 1731–1736 (2006).
10. State Standard GOST 27637-88: Self-Finished Products from Aluminum Deformed Thermo-Hardening Alloys. Control of Dead-Burning by Metallographical Method (Izd-vo Standartov, Moscow, 1988).
11. W. C. Oliver and G. M. Pharr, "An improved technique for determining hardness and elastic modulus using load and displacement sensing indentation experiments," Mater. Res. **7**, 1564–1583 (1992).
12. Yu. I. Golovin, Nanoindentation and its Possibilities. Mechanical Engineering. (Mashinostroenie, Moscow, 2009) [in Russian].
13. Yu. V. Mil'man, K. E. Grinkevich, and L. V. Mordel', "The energy concept of hardness upon instrumental indentation," Deform. Razrush. Mater. **2013**, 2–9 (2013).
14. K. V. Gogolinskii, N. A. L'vova, and A. S. Useinov, "Application of scanning microprobe analysis and nanodurometers to the study of the mechanical properties of solids at a nanolevel," Zavod. Lab., Diagn. Mater. **73**, 28–36 (2007).
15. G. Leibfrid, "Microcsopic Theory of Mechanical and Thermal Properties of Crystals," in Handbuch der Physik (Springer, Berlin, 1955; Fizmatgiz, Moscow, 1963), Vol. VII, part 2.
16. Yu. I. Golovin, "Nanoindentation and mechanical properties of solids in submicrovolumes, thin near-surface layers, and films: A review," Phys. Solid State **50**, 2205–2236 (2008).
17. S. I. Bulychev, "Relation between the reduced and unreduced hardness in nanomicroindentation tests," Tech. Phys. **44**, 775–781 (1999).
18. S. V. Miroshnichenko, "Dispersion of the billet hardness as a criterion of optimality for accumulated strain," Fiz. Tekh. Vys. Davlenii, **15**, 72–75 (2005).
19. W. Yang, S. Ji, X. Zhou, I. Stone, G. Scamans, G. E. Thompson, and Z. Fan, "Heterogeneous nucleation of α-Al grain on primary α-AlFeMnSi intermetallic investigated using 3D SEM ultramicrotomy and HR TEM," Metall. Mater. Trans. A, **45**, 3971–3980 (2014).
20. M. Poková, M. Cieslar, and J. Lacaze, "The influence of silicon content on recrystallization of twin-roll cast aluminum alloys for heat exchangers," Acta Phys. Polon. A **122**, 625–629 (2012).
21. O. A. Chikova, E. V. Shishkina, A. N. Petrova, and I. G. Brodova, "Measuring the nanohardness of commercial submicrocrystalline aluminum alloys produced by dynamic pressing," Phys. Met. Metallogr. **115**, 523–528 (2014).
22. N. I. Muskhelishvili, Some Basic Problems of Mathematical Theory of Elasticity (Nauka, Moscow, 1966) [in Russian].
23. I. N. Frantsevich, F. F. Voronov, and S. A. Bakuta, Elastic Constants and Metal and Nonmetal Modules of Elasticity. A Hanfbook (Naukova Dumka, Kiev, 1982) [in Russian].
24. H. B. Huntington, "The Elastic Constants of Crystals," in Solid State Physics : Advances in Research and Applications, **7**, 213-351 (1958).
25. A. I. Yurkova, A. V. Belotskii, A. V. Byakova, and Yu. V. Mil'man, "Mechannical properties of nanostructural iron obtained by severe plastic deformation by friction," Nanosyst., Nanomater., Nanotechn. **7**, 619–632 (2009).
26. S. A. Firstov, V. F. Gorban', and E. P. Pechkovskii, "Measurement of ultimate values of hardness, elastic strain and stress of materials by an automatic indentation method," Materialovedenie, No. **8**, 15–21 (2008).

Translated by D. Tkachuk